NASA TECHNICAL MEMORANDUM

NASA TM X-71782

NASA TM X-71782

(NASA-TM-X-71782) EXPERIENCE WITH INTEGRALLY-CAST COMPRESSOR AND TURBINE COMPONENTS FOR A SMALL, LOW-COST, EXPENDABLE-TYPE TURBOJET ENGINE (NASA) 39 p HC $3.75 CSCL 21E G3/07

N75-30175

Unclas 34273

EXPERIENCE WITH INTEGRALLY-CAST COMPRESSOR AND TURBINE COMPONENTS FOR A SMALL, LOW-COST, EXPENDABLE-TYPE TURBOJET ENGINE

by Robert P. Dengler
Lewis Research Center
Cleveland, Ohio 44135

TECHNICAL PAPER to be presented at the
1975 Aerospace Engineering and Manufacturing Meeting
sponsored by the Society of Automotive Engineers,
Los Angeles, California, November 17-20, 1975

EXPERIENCE WITH INTEGRALLY-CAST COMPRESSOR AND TURBINE COMPONENTS FOR A SMALL, LOW-COST, EXPENDABLE-TYPE TURBOJET ENGINE

Robert P. Dengler

National Aeronautics and Space Administration
Lewis Research Center
Cleveland, Ohio 44135

E-8441

ABSTRACT

A discussion regarding experiences with integrally-cast compressor and turbine components during fabrication and testing of four engine assemblies of a small (29 cm ($11\frac{1}{2}$ in.) maximum diameter) experimental turbojet engine design for an expendable application is presented. Various operations such as metal removal, welding, and re-shaping of these components were performed in preparation of full-scale engine tests. Engines with these components have been operated for a total of 157 hours at engine speeds as high as 38,000 rpm and at turbine inlet temperatures as high as 1256 K (1800° F).

EXPERIENCE WITH INTEGRALLY-CAST COMPRESSOR AND TURBINE COMPONENTS FOR A SMALL, LOW-COST, EXPENDABLE-TYPE TURBOJET ENGINE

Robert P. Dengler

National Aeronautics and Space Administration
Lewis Research Center
Cleveland, Ohio 44135

E-8441

SUMMARY

The design of a small, low-cost, experimental turbojet engine for an expendable-type application was used for fabricating and assembling a total of four engines. This design incorporated some low-cost concepts that were under study at NASA-Lewis. One of the primary low-cost principles found in the design was that of utilizing integrally-cast engine components; in particular, those for the compressor and turbine sections. Integral disk-blade rotors of approximately 20 centimeters (8 in.) diameter were precision investment cast from 17-4 PH material for the four-stage axial-flow compressor. The individual rotors and a cast 17-4 PH hollow shaft were joined by circumferential electron beam welding. The welded assembly was attached through a bolted connection to an integrally-cast IN-100 disk-blade turbine rotor of approximately 24 centimeters ($9\frac{1}{2}$ in.) diameter. The turbine stator ring was produced as a one-piece investment casting from Stellite 31 material, and the individual compressor stator vanes were cast from 17-4 PH. Experiences with regards to the integrity of these cast components during fabrication procedures and as a result of engine operation are discussed. A variety of fabrication-type operations such as metal removal, welding and re-shaping by bending and twisting were performed on these cast components. Engines with these components have been operated for a total of 157 hours at sea level static and a range of simulated flight conditions with engine speeds as high as 38,000 rpm and turbine inlet temperatures as high as 1256 K (1800° F).

INTRODUCTION

The small size and weight of the gas turbine engine makes it attractive for use in missile applications, but the very high cost of current gas turbine engines restricts their use. Substitution of small, low-cost gas turbine engines for rocket engines presently used on some missile applications appears particularly attractive because it would extend or improve the payload range and capability as well as result in a significant cost savings. The very short life requirement and relatively high fuel consumption allowance of engines for drones and missiles makes possible considerable major simplifications in the construction of such engines.

The basic design of a low-cost engine should incorporate inherent economical approaches and yet be simple in concept; more specifically, the use of costly materials and fabrication methods must be kept to a minimum. By nature, this premise generally implies a compromise trade-off of performance for lower costs; usually resulting in a somewhat higher specific fuel consumption or lower specific thrust. For the application being considered however, this performance trade-off can be seen as being generally acceptable.

A complete design for a small, expendable-type turbojet engine was generated under NASA contract (refs. 1 and 2) and subsequently used for fabrication purposes. The design was subject to some requirements submitted by the Naval Weapons Center at China Lake, California who intended using the engines for flight tests to demonstrate the feasibility of replacing rocket engines in missile applications. The significant intent or overall objective was for this engine to be a demonstrator of some low-cost concepts that were under study at NASA-Lewis Research Center (see refs. 3, 4, and 5).

One of the primary low-cost principles found in this engine design is that of utilizing one-piece precision castings to reduce and minimize costly machining operations and to eliminate the need for welded flanges or other parts. The majority of the larger components for this engine were produced through some type of casting process. Included in this category were the most critical of the engine parts, the

compressor and turbine components which were precision investment cast. 17-4 PH material was used for the compressor's stator vanes and integral blade/disk assemblies, Stellite 31 for the integral turbine stator assembly, and IN-100 for the integral blade/disk turbine rotor. Another significant feature of this design was an all-welded compressor rotor mainshaft assembly which consisted of just four circumferential electron beam welds to join the hollow cast rotor mainshaft and the integrally-cast rotor stages together.

This report presents some experiences encountered at NASA-Lewis with integrally-cast compressor and turbine components from the investigation of this small, low-cost experimental turbojet engine. During fabrication and assembly, or as a result of desired design modifications, a variety of machining, forming and welding operations along with heat treating cycles were performed on the integrally-cast compressor and turbine components. A discussion of these operations are presented herein along with comments and/or conclusions with respect to the machinability, formability, workability, and weldability of materials used for these components. Engines with these integrally-cast components have been operated at speeds up to 38,000 rpm (8 percent above design speed) and at turbine inlet temperatures as high as 1256 K (1800° F). Comments are also made with respect to the structural integrity of these components as a result of actual test operations.

ENGINE DESIGN AND DESCRIPTION

This section describes the turbojet engine design that was generated for the purpose of providing the Naval Weapons Center with an experimental engine of the expendable-type for a flight test to demonstrate the feasibility of replacing the rocket engine in a missile application. The basic requirements of this engine were that it be:

(1) Small in size - on the order of 30 centimeters (12 in.) in diameter and 97 centimeters (38 in.) in length,

(2) Relatively light in overall weight - approximately 54 kilograms (120 lb),

(3) Capable of air launch from windmilling condition at altitude,

(4) Capable of producing 2669 newtons (600 lb) of thrust at sea level static conditions,

(5) Capable of producing 1646 newtons (370 lb) of thrust at its cruise condition of a flight Mach number of 0.8 and an altitude of 6096 meters (20,000 ft), and

(6) Self-sufficient and capable of a mission with a flight duration of 20 minutes.

A cross-sectional view of the engine design generated is shown in figure 1. This axial-flow turbojet engine design consists of a four-stage compressor, an annular combustor, a single-stage turbine and a fixed area exhaust nozzle. Significant features of the design include:

(1) Compressor and turbine rotor disks cast integrally with their respective blading,

(2) An integrally-cast compressor inlet and front main bearing support,

(3) An all-welded (including individual stages) compressor-rotor mainshaft assembly,

(4) A simplified perforated combustor liner,

(5) Simplex fuel nozzles for the combustor, of the same type as those used in oil-burning furnaces,

(6) An integrally-cast turbine exhaust casing and rear main bearing housing,

(7) An integrally-cast (360^{o} (one-piece)) turbine stator assembly,

(8) A compressor-turbine rotor mainshaft assembly that was simply supported through a soft-mounted, two-bearing system,

(9) An oil-mist bearing lubrication system, and

(10) A simplified fuel pump/fuel control assembly.

These features together with the economical application of materials and manufacturing processes contribute toward the low production-cost potential of this engine design. The extensive use of casting processes for providing the majority of the major components of this engine is illustrated by figure 2. It was intended to obtain maximum utilization of "as cast" surfaces, and also maximum use of simple turning

(machining) operations along with a minimum use of cores. In addition, a liberal airfoil profile tolerance was allowed for the compressor and turbine components. The penalty for this dependency on castings was additional weight due to the heavier-than-normal components. Although the purpose of the investigation was to demonstrate the feasibility and validity of all these basic design concepts or simplifications, the remainder of this report will concentrate only on the integrally-cast components in the engine's compressor and turbine sections.

Compressor Components

The compressor rotor mainshaft assembly was of an all-welded design and consisted of a cast hollow rotor shaft and four separate and integrally-cast solid blade/disk rotor stages, all of which were cast from 17-4 PH (AMS 5355), a heat-treatable, high strength, ferrous alloy of relatively low cost and good machinability. (Table I lists the chemical composition for this and other pertinent materials.) Figure 3 compares the compressor rotor components in the "as cast" condition with similar components after "dress-up" machining in preparation for subsequent balancing and welding operations. The mean blade tip diameter for the four rotor stages was about 20 centimeters (8 in.). This and other pertinent dimensions for the hub and tip sections of airfoils for the compressor and turbine components are provided in table II.

The actual design for the compressor stator calls for utilizing two 180° integrally-cast aluminum vane and shroud assemblies for each of the four compressor stator stages. It was decided, however, to provide the compressor with individual stator vanes that could be adjusted if necessary for obtaining the optimum vane setting angles. It was intended that subsequent engine assemblies would incorporate the integrally-cast split ring stator assemblies with vanes cast to the desired setting angle. The individual solid vanes used in the test engines were precision cast from the same ferrous alloy, 17-4 PH, as used for the compressor rotor components.

Figure 4 shows a cast vane from each of the four stages in the compressor section. The cast stub (stem) at one end of the vane was machined to provide threading for ease of mounting to the compressor casing with the locknut shown on the threaded portion. Flat surfaces were machined on the stem of the stator vanes to allow for orienting and adjusting the vane setting angle.

Even though the intent was to make maximum utilization of "as cast" surfaces, the limitations of normal casting processes required that liberal tolerances be employed in order to assure a respectably high casting yield percentage. The following tolerances were specified for castings of the respective components:

Compressor and turbine rotor stages:

(1) General casting tolerance of ±0.005 centimeter/centimeter (in./in.) with a maximum of ±0.051 centimeter (0.020 in.)

(2) Airfoil section contour maintained within a band of -0.000 to +0.013 centimeter (+0.005 to -0.000 in.) tolerance parallel to the nominal (design) contour

Compressor and turbine stator stages:

(1) General casting tolerance of ±0.005 centimeter/centimeter (in./in.) with a maximum of ±0.051 centimeter (0.020 in.)

(2) Airfoil section contour maintained within a band of +0.015 to -0.000 centimeter (+0.006 to -0.000 in.) tolerance parallel to the nominal (design) contour

Turbine Components

The single-stage axial-flow turbine consisted of a stator vane assembly and a bladed rotor assembly. A comparison of these components in the "as cast" condition with similar components in the chined version ready for assembly is shown in figure 5. The stator vane assembly consists of 35 radially-tapered solid airfoil-shaped vanes between two shroud rings and was cast from Stellite 31 (AMS 5382)

material (see table I) as an integral (one-piece) 360° component. The outer shroud ring of this casting extends rearward past the plane of the vane trailing edge to form the stationary shroud for the turbine rotor blades. The turbine rotor is an integrally-cast solid rotor blade and disk assembly incorporating 57 radially-tapered turbine blades and a stub shaft which becomes the surface for the rear bearing. The six through-holes seen in the finished rotor is for bolting the turbine to the compressor rotor mainshaft. The material used for producing the turbine rotor castings was IN-100 (AMS 5397), a high-temperature, high-strength nickel alloy (see table I). The blade tip diameter of the turbine rotor after machining was about 24.5 centimeters (9.65 in.). At the maximum operating speed of 38,000 rpm, this results in a tip speed of 487 meters per second (1600 ft/sec).

DISCUSSION

This section of the report will concentrate on a discussion of various operations performed on the integrally-cast compressor and turbine components during this engine investigation. A discussion of the structural integrity of these components during engine tests is also included in this presentation. The engine performance data resulting from this investigation will be presented in a separate report and therefore are not included as a part of this report. Four engines were assembled and tests were conducted over a range of engine speed up to 38,000 rpm and at turbine inlet temperatures as high as 1256 K (1800° F) at both sea level static and for a range of simulated flight conditions that covered flight Mach numbers up to 1.2 and altitudes up to 9144 meters (30,000 ft). A total of 157 hours of test time had been accumulated on the four engine assemblies. Figure 6 shows one of the two engine assemblies that were shipped to the Naval Weapons Center for their demonstration tests.

Compressor Components

When castings of these components were received they were subjected to the normal inspection procedures which included dye penetrant checks and radiographic examinations for cracks and voids, along with a dimensional verification. Only a very few castings were found to have unacceptable flaws such as cracks or voids. The airfoil section contours of the castings were generally found to be within the allowable tolerance band, but they were almost always on the thick side and in some cases just beyond the maximum allowed in the specifications.

Solution treatment of 17-4 PH castings. - Prior to any machining on the compressor castings, the castings were subjected to a double solution treatment at 1311 K (1900° F) in lieu of a usual treatment of homogenizing at 1422 K (2100° F) followed by a single solution treatment at 1311 K (1900° F). As pointed out in reference 6, the double solution treatment is effective in refining grain size and improving ductility and impact strength. The procedure for solution treating then was to charge the castings into a furnace within an argon atmosphere retort at a temperature of 1311 K (1900° F) for 1/2 hour, after which the castings were cooled down to a temperature of 700 K (800° F) while still in the argon atmosphere, and then cooled in air to 367 K (200° F) and finally water quenched to room temperature (at least below 306 K (90° F)). This cycle was repeated to provide the double solution treatment (condition A). The argon atmosphere was used to prevent any scaling of surfaces that were to be used "as cast".

All-welded compressor rotor-mainshaft assembly. - Figure 7 shows a schematic of the compressor components before welding and also presents a detailed view of the machined geometry of mating flange rims used to obtain dependable welds. The objective was to provide a concentric surface of uniform thickness on the order of 0.229 centimeter (0.090 in.). The "step" design provides an excellent way of aligning the two adjacent rotor stages for the welding operation to assure that the above conditions of concentricity and uniform thickness are obtained where the welded joint is required.

Following a balancing of all individual components and prior to any electron beam welding, these 17-4 PH castings were subjected to a de-magnetizing operation. Early experimental test welds on this material had shown that the magnetic properties of the material caused a deflection of the electron beam during the welding process.

The rotor mainshaft was installed and aligned in the chuck of the welder's mounting fixture and the fourth stage rotor was then aligned with the mainshaft and held in place by a spring arrangement that exerts a force of about 178 newtons (40 lb). Figure 8 provides a close-up view of the two components in the mounting fixture after the first electron beam welding operation. The procedure used for welding was to first make spot welds at about eight equally spaced locations around the circumference. After this was completed, a "clean-up" pass or partial penetration of about 0.025 centimeter (0.010 in.) depth was made for one complete revolution of the work pieces in order to clean and also preheat the weld region Then, a full penetration weld was made for one complete revolution plus about a 5-centimeter (2-in.) overlap. For a 0.236-centimeter (0.093-in.) wall thickness the conditions or settings for a full penetration weld in this 30 kw Sciaky Electron Beam Welder were:

Kv = 25.6
Ma = 54
Focus = 600

} For a 10-centimeter (4-in.) working distance

All welds were made at a rate of 2.5 centimeters per second (1 in./sec) so that the entire circumferential weld joining the rotor mainshaft to the fourth stage rotor was accomplished in a total of about 20 seconds. The weld bead resulting from the full penetration weld was on the order of 0.08 centimeter (1/32 in.) in width. A final "wash" pass was made for one full revolution to smooth out the ridge left by the full penetration weld. The electron beam was slightly de-focused in the "wash" pass and resulted in an affected zone width of about 0.32 centimeter (1/8 in.) on the surface.

Also shown in figure 8 is a cylindrical test specimen of similar material and thickness which was used as a practice piece in determining the proper settings for a

full penetration weld. The other three rotor stages were subsequently welded together in a similar manner to complete the compressor rotor mainshaft assembly. Figure 9 shows a rotor assembly after all welding operations had been completed.

Prior to any welding, all the components were stacked in a vertical arrangement to obtain pertinent measurements such as stacked height, shaft surface run-outs, and axial run-out at the upstream face of the first compressor rotor stage. After each weld operation, similar measurements were recorded. In most cases, any undesirable axial run-out caused by weld shrinkage could be compensated for or at least partially corrected for by judiciously choosing the location (circumferentially) and length of a subsequent weld overlap which causes additional shrinkage in that region. In a case where the axial run-out was considered excessive, the welded units were removed and this surface was re-machined in a lathe to correct the run-out. The axial run-outs resulting from welds usually did not exceed 0.013 centimeter (0.005 in.) and generally were no more than 0.008 centimeter (0.003 in.). The difference in stacked height before and after all welding operations for a typical assembly was 0.067 centimeter (0.0265 in.) which yields an average shrinkage of 0.0168 centimeter (0.0066 in.) per weld. Needless to say, these shrinkages must be anticipated and allowed for during dress-up machining of these parts prior to any welding. After completing the last weld on the rotor assembly shown in figure 9, the total axial run-out at the front face of the first rotor stage was 0.0038 centimeter (0.0015 in.).

Because the time for each weld was very short and the electron beam is so concentrated, the heat-effected zones of the components were very limited and therefore no re-solutioning treatment was required.

Age-hardening treatment for 17-4 PH components. - All 17-4 PH components were age-hardened through a heat treatment to condition H 1025. In the case of the rotor assembly, the aging treatment was performed after all welding operations but prior to the final machining operations on the bearing and seal surfaces. The components were exposed to a temperature of 825 K (1025° F) in a furnace with an

air atmosphere for a period of 4 hours and subsequently air-cooled to room temperature. The higher aging temperature of 825 K (compared to 756 K (900° F) for maximum strength) has the effect of increasing ductility, toughness, and resistance to stress corrosion cracking at the expense of lowering (by about 9 percent) the strength properties. A dimensional check after aging revealed that the assembly had shrunk about 0.043 centimeter (0.017 in.) in length or "stacked height". This shrinkage or contraction rate compares favorably with the value of 0.0007 centimeter/centimeter (in./in.) listed in the Aerospace Structural Materials Handbook (ref. 7) at this aging temperature.

Modifications to blade and vane aerodynamic characteristics. - The results of a series of full-scale engine testing with the first set of compressor components revealed some deficiencies in the performance of the compressor. It was subsequently decided to make an attempt to correct these deficiencies by altering the blade section profiles or aerodynamic characteristics.

Chemical milling: Although the "as cast" airfoil section profile contours were generally within specified tolerances with respect to the maximum allowable "thickness", it was nevertheless found desirable to reduce the overall thickness, particularly in the leading and trailing edge regions, to better simulate the geometry for the nominal or design contours. The method selected to produce the desired results was chemical contour machining or what is more commonly referred to as chemical milling. The etchant or chemical bath solution selected for this machining operation was the standard etchant solution listed for stainless steel in reference 8 (the Metals Handbook); the formula for which consisted of the following ingredients:

HCl - 50 percent by volume

HNO_3 - 5 percent by volume

H_3PO_4 - 2.5 percent by volume

H_2O - 42.5 percent by volume

Figure 10 shows the apparatus used for chemical milling the rotor blades and stator vanes. Using this apparatus, a single rotor stage or as many as 42 stator

vanes could be machined in one operation. Those surfaces where chemical milling was undesirable, were masked off (not shown in the figures) with a standard commercial maskant or mylar tape. The general procedure was to fill the plexiglas container with about 4 liters of the etchant solution and then to place the plexiglas container inside the stainless steel container. The gap between the containers was then filled with water, and the steel tank placed on a hotplate. The bath solution was heated and controlled to a temperature of 344 K (160° F) and the components to be machined were rotated in the bath solution at a speed of about 35 rpm through the use of the electric motor shown in the figure. Using this technique, the blade or vane profile contour (thickness) was reduced by as much as 0.041 centimeter (0.016 in.) (0.020 cm on a surface). It was found that a 4-liter batch of the solution would "exhaust" itself after about 28 cubic centimeters (1700 sq in. - mils) of metal removal, and the rate of metal removal was about 0.0025 centimeter (0.001 in.) in 4 to 5 minutes. This removal rate is slightly lower than the value of 0.00076 centimeter per minute (0.0003 in./min) listed in reference 8 (Metals Handbook) for stainless steels. The resulting surface finish was as good or better than the original "as cast" surface. Profiles of some blade section contours were obtained with the use of a blade plotting machine. The machine was used to produce 10 x size "eyelash"-type profiles on sheets of Mylar film. Figure 11 presents an overalay of two Mylar plots (before and after chemical milling) for the same blade section to reveal the uniformity of this metal removal method. For the typical case presented, the surface removal was approximately 0.015 centimeter (0.006 in.) in thickness.

For applications using integrally-cast rotor blade/disk assemblies requiring extra thin airfoil leading and trailing edges, chemical milling may prove to be very appropriate and useful. Normal casting processes are usually very limited and result in low percentage casting yields when thin sections are required, even when resorting to a vibrating or centrifugal casting technique. By judiciously designing "thicker" blade contours which can be more easily cast, they could subsequently be "thinned" through chemical milling. No specific application is implied herein, nor has any economic study been made as to the practicality of this method for

producing a finished product. It does appear, however, that this method warrants further consideration.

Re-shaping blade airfoils: In the course of conducting preliminary full-scale engine tests, it was found desirable to further alter the aerodynamic characteristics of the blading for the compressor rotor stages. These changes amounted to a re-shaping of the blading to effect a change in the blade setting angle or blade camber angle. A typical blade section is shown in figure 12 to illustrate the angles of interest. Re-cambering of individual solid vanes or blades (not integrally cast with disk) can normally be accomplished through fabricating appropriate dies and forcefully forming the airfoils to the newly desired shape. However, it obviously becomes somewhat more difficult to accomplish when the blades are integral with the rotor disk. If this engine were being considered for production, a modification of the casting dies would be warranted to achieve the desired changes. However, since the program schedule did not allow for any lengthy time delays, it was decided to affect these changes in-house in a manner considered to be most expeditious. The objective, then, was to rely on simple tooling which would not require lengthy design or fabrication procedures and yet produce the desired results. With this in mind, a series of tools were fabricated (see fig. 13) for firmly gripping individual airfoils on each integrally-cast rotor stage to effect the desired angle changes.

When blade camber angles were to be changed, the tooling took the form of pins mounted to a flat piece of barstock material $1.3 \times 2.5 \times 25.4$ centimeter ($1/2 \times 1 \times 10$ in.) in length. Figure 14 shows a close-up view of a typical set-up for changing the blade camber angle in the trailing edge region of the blade. A second stage rotor is shown mounted on the table of a milling machine (used as stationary fixture only) and the pins of the forming tool placed over the blade with one pin on each side of the blade ready for the bending operation. One of the pins extends through the barstock and is held in the spindle of the milling machine and becomes the pivoting center for the barstock which is used as a lever arm. A makeshift graduated scale (in degrees) is attached to the "head" which houses the

spindle and a pointer is " attached" to the lever arm to provide an indication of angle change that occurs. For the bending operation set-up as shown in figure 14, the bending occurs from the approximate midchord region of the airfoil back to the trailing edge. If a camber angle change was required in the leading edge region, a similar bending operation was performed. Although it was obvious that angle changes would have to be limited when approaching a section near the blade-to-disk joint of the integral casting, angle changes on the order of 5^{o} were still possible at a region of only 0.38 centimeter (0.15 in.) above the blade-disk joint for the third and fourth stage blading. At the same blade span for the first and second stage blading, practically no angle change (about $1/2^{o}$) was possible with this tooling. (The first and second stage blading was somewhat thicker than that of the third and fourth stages.) Figure 15 presents some overlays of "eye lash" profiles (from blade plotter) for the hub, midspan, and tip sections of a fourth stage rotor blade (before and after) to indicate the camber angle change after a dual bending operation. The table accompanying the profiles lists the camber angles before and after bending. Total blade camber angles were changed by as much as 7^{o} in the blade tip region. The average time required to affect blade camber angle changes for a complete rotor stage was about one working day (8 man-hr). If, upon subsequent full-scale engine testing it was found that additional re-cambering or even de-cambering was required, these new changes were accomplished with the same tooling.

For altering the setting angle of the blade, the tooling either conformed to the blade surface contour or was constructed to slide over the blade to firmly grip the blade along almost the entire span of the leading and trailing edge as well as at a section near the blade base. Figure 16 presents profile overlays (before and after twist) for the hub and tip sections of a first-stage rotor blade showing the amount of twist affected. If blade setting angles were determined to be within $\pm 0.5^{o}$ of the desired setting angle, the twist operation was considered successful. Otherwise, those blades not within this tolerance would be re-twisted until acceptable. Blade setting angles at the tip section were changed by as much as 5^{o} using this technique.

Normally, only a limited number of blades from each stage were selected for profiling (at several blade sections) on the blade plotter to determine whether the angle changes for the bending or twisting operations were correct. The blade tip angles for all the blades, however, were checked using an optical comparator. Minor blade angle changes in the tip region could be made with a pair of vise grips while the blade tip angle was still being checked in the comparator. A considerable amount of bending and twisting operations (angle changes) were performed for the four engine assemblies without detecting any cracks through radiographic or dye penetrant inspection methods following these operations.

Turbine Components

Stator. - Initial testing with the first engine assembly revealed a mismatch of flow characteristics between the compressor and the turbine. As a result, a decision was made to increase the stator throat area to a value of 5 percent over that of the design value. Since the turbine stator castings (as received) had throat areas that were generally 5 percent under the design value, this, then, meant a required change in area of 10 percent.

A special tool, shaped to the contour of the vane's pressure (concave) surface was used in conjunction with the compression head of a tensile testing machine to forcefully open up the throat area (in the trailing-edge region) to the desired value. Figure 17 shows the set-up with the shaped tool just above the turbine stator assembly prior to engaging it with the pressure surface of a vane for an "opening" operation. A dial indicator was used for measuring the movement of the compression head which, in turn, provided a method for gaging the required amount of throat enlargement.

This throat opening process usually resulted in producing cracks in the vane trailing edge near the filleted regions of the inner and outer shroud rings. Center-punch marks were put at the end of the cracks so that a record of any crack propagation could be made at periodic intervals of engine testing. Although a crack did

initiate in the midspan leading edge region of a few turbine stator vanes as a result of testing at average turbine inlet temperatures calculated to be as high as 1256 K (1800° F) the trailing edge cracks initiated by throat opening operations did not show any evidence of propagating.

Rotor. - Because integral castings can present problems not normally encountered, the turbine rotor was subjected to careful and thorough design procedures including that of stress and vibration analyses. Since integral castings of this nature possess an inherent lack of damping qualities, special attention was directed towards avoiding any critical or resonant frequencies of the turbine blade with respect to bending and torsional modes over the range of speeds for engine operation. Figure 18 presents a reproduction of the turbine blade interference diagram generated for this engine design with curves of selected engine order excitation frequencies superimposed. The fundamental natural frequencies for the bending and torsional modes for the turbine rotor blade were calculated to be about 3170 and 5170 hertz, respectively. The analysis treated the blade as a cantilever beam fixed at the rim of the disk.

In addition to the 1 and 2 per rev excitation frequencies normally generated by the engine, the other engine orders of significant interest would be 3 and 35 since there were three struts downstream, and 35 stator vanes upstream of the rotor. According to the diagram, none of these engine orders should present any critical resonance problems with respect to the first mode bending over the range of speeds from 7000 rpm (windmilling speeds for engine starts at sea level static) to the maximum operating speed of 38,000 rpm. The 35 engine order does intercept the first mode torsion critical frequency at about 9000 rpm, but upon engine start the speed is quickly accelerated through this speed regime to an idle speed of at least 25,000 rpm.

Despite the precautions taken in both design and inspection procedures, a turbine rotor did suffer a blade failure after about 35 hours of intensive, full-scale engine testing. The blade had fractured at a span dimension of about 0.6 centimeter (1/4 in.) from the integral blade-to-disk joint. Figure 19 shows a view of the fractured surface of the portion of blade remaining with the rotor disk. A post-test

inspection of the turbine rotor revealed that five other blades had chordwise cracks in the trailing edges at approximately the same span distance. Figure 20 shows the downstream side of the turbine rotor with blades having cracked trailing edges. Figure 21 shows a closeup view of the trailing edge of blade 21 clearly revealing the crack which had already propagated for a distance of about 0.95 centimeter (3/8 in.).

A microscopic inspection of the fractured surfaces for the failed blade and the "cracked" blades revealed "beach" marks which are highly suggestive of a fatigue failure and most likely that of a high-cycle mode.

In an attempt to resolve the cause of failure, vibration tests were conducted on an individual blade and an entire turbine rotor. One general purpose of these tests was to verify the calculated values for the fundamental natural frequencies of the blading for the bending and torsional modes. Another purpose was to take advantage of this technique for determining highly stressed regions of the blade for strategic placement of strain gages for rotative tests, if so desired.

A series of hologram-photographs were obtained from the vibration tests using a laser light to reveal the vibration mode stress concentration patterns at selected excitation frequencies. Figure 22 shows a typical arrangement of the apparatus used for producing the holograms. The equipment includes a laser light with associated lenses and mirrors, a small "shaker" (vibration exciter), and an air (floating) table. The camera used to record the holograms is not shown, and the blade mounted on the shaker is from another investigation.

An individual turbine rotor blade was "sliced" from a turbine rotor wheel (with a sufficient portion of the disk), mounted in the shaker, and excited to resonant frequencies. A series of holograms were produced and are shown in figure 23 for general interest. This technique of time-average holography not only defines the first mode critical bending and torsional frequencies but also reveals other vibration modes that are not analytically predicted. The properties of holograms are such that they reconstruct images of the vibrating object marked by dark fringes,

any of which represents points of specific vibration magnitude. The dark fringes are separated by bright fringes, whose brightness decreases with increasing vibration amplitude. This latter effect provides a way to interpret photographs of the reconstructed images in the manner of topographical maps. According to reference 9 the vibration amplitude at object points that are covered by dark fringes is very nearly proportional to the order number of dark fringes minus 1/4. The strong or pronounced patterns produced in holograms of figure 23(c) (3125 Hz) and figure 23(d) (5888 Hz) seem to indicate that they represent critical resonant frequencies for first mode bending and torsion, respectively. The value of 3125 hertz compares favorably with the value of 3170 hertz that was calculated for the first mode bending on the interference diagram of figure 18 but the value of 5888 hertz is somewhat higher (by about 14 percent) than the value shown in the figure for the first mode torsion. The noticeable difference in these latter values might be accounted for by the fact that the analysis used the airfoil design contour while the actual cast blade was somewhat thicker.

The bright region of the holograms represents the locus of points of zero displacement and by counting the interference fringes towards the tip of the blade one can compute the relative displacement of any point on the blade. The areas of maximum stress can then be determined from these patterns which can be helpful in defining optimum locations for application of strain gages for monitoring purposes during rotative tests if further verification is warranted.

An entire turbine rotor assembly was subsequently mounted to the shaker (see fig. 24) and excited to resonant frequencies to produce the series of hologram-photographs shown in figures 25(a) through (f). The resonant frequencies are listed with each hologram. The rotor was centrally supported, and mounted similar to the manner in which it would be for an engine assembly (six through-bolts), and vibrated along its horizontal axis. According to reference 10 the vibration modes can be classified by the number of diametral mode lines, and the holograms presented are so classified.

Although probably coincidental, it was observed that the general pattern or location of cracked blades (including the fractured one) on the rotor (see fig. 20) resembled the pattern of the 3-diameter modes for the excitation frequencies of 2737 and 4266 hertz (figs. 26(b) and (e), respectively). Furthermore, it was noticed that the cracked blades of the rotor and the "nodal" blades of the hologram for 4266 hertz appear to be very nearly in line with the six bolt holes for attaching the rotor to the compressor rotor mainshaft assembly.

Although no apparent potential problems were indicated on the interference diagram with respect to a three-excitation order, the effect of the three struts located about 3.2 centimeters ($1\frac{1}{4}$ in.) downstream of the turbine rotor has since become suspect. It has been hypothesized that a resonant frequency of a lesser excitation order for integral castings, such as the turbine rotor, could result in producing a higher excitation order effect. For this particular rotor, it is suggested that the second harmonic of a three-excitation order (three struts in tailcone) could still be strong enough to conceivably produce a six-excitation order effect It can be seen from the interference diagram (fig. 18) that the six-excitation order curve crosses the critical frequency for the first bending mode in the region where most of the engine operation was conducted; that is, between 30,000 and 38,000 rpm. With the blades being cast integral with the rotor disk, the damping characteristics at the blade root are considered minimal. This being the case, a significant resonance might very well appear as a result of a lesser excitation order, but there is no known way of predicting the vibration level except through actual experience. Once this premise is accepted, the excitation frequency of 3064 hertz which produced the wheel hologram of figure 25(c) becomes highly suspect. The hologram results in a complex stress pattern having an elliptical shape with the locus of points of zero displacement (bright region) traversing the disk portion of the rotor and extending outward into the blade roots. This excitation frequency is close to the predicted value for the fundamental natural frequency for the first mode bending of the blade. If the second harmonic of a three-engine order effect did, indeed, produce a six-excitation order effect it is conceivable that a resonant frequency could have resulted at an engine speed of 30,640 rpm.

Although the vibrational study was not conclusive with regards to the probable failure mode, the resulting holograms provided some interesting and enlightening information. The unknown aspects of the failure mode do point up the continuous need for rigorous analysis and engine developmental testing before new engine designs are certified for long-time service or man-rated applications.

CONCLUDING REMARKS

The four engines assembled for this investigation were operated over a wide range of simulated test conditions with turbine inlet temperatures as high as 1256 K (1800° F) and rotor speeds up to 38,000 rpm for a total of 157 hours. Two complete engine assemblies were delivered to the Naval Weapons Center for their demonstration testing purposes. After initial operational problems were resolved, the engine design was considered more than adequate for the purpose intended. The choice of materials for the integrally-cast compressor and turbine components proved to be based on sound judgment, despite the unresolved blade failure in one turbine after 35 hours of intensely varied operation. The cast 17-4 PH material used in the compressor components was subjected to a variety of fabricational procedures and proved to have very good machining (conventional and otherwise), forming, and electron beam welding qualities. In addition, these compressor components withstood many hours of operation without blade failures or evidence of stress corrosion cracking.

REFERENCES

1. C. Ellis, R. Jaklitsch, A. Leto, and R. Schaefer: Design of the NASA Simplified Turbojet Engine C. Rep. CW-WR-69-057.F, Curtiss-Wright Corp., July 1969. (Contract NAS 3-12423.)

2. C. Ellis, A. Leto, and R. Schaefer: Compilation of Preliminary Design Data on Ordnance Engine. Rep. CW-WR-70-074, Curtiss-Wright Corp., Sept. 1970. (Contract NAS 3-12423.)

3. R. L. Cummings and H. Gold: Concepts for Cost Reduction on Turbine Engines for General Aviation. NASA TM X-52951, March 1971.

4. R. L. Cummings: Experience with Low Cost Engines. NASA TM X-68085, March 1972.

5. Harold Gold: A Simplified Fuel Control Approach for Low Cost Aircraft Gas Turbines. NASA TM X-68229, April 1973.

6. Anon.: Armco 17-4 PH: Bulletin, Armco Steel Corp., Sept. 1969.

7. Air Force Materials Information Center: Aerospace Structural Metals Handbook. AFML-TR-68-115, 1975 Publication.

8. American Society for Metals: Metals Handbook (Vol. 3, Machining), 8th Edition, Copyright, 1967.

9. K. A. Stetson and P. A. Taylor: The Use of Normal Mode Theory in Holographic Vibration Analysis with Application to an Asymmetrical Circular Disk, Journal of Physics E, Scientific Instruments, 1971, Volume 4, pp. 1009-1015.

10. K. A. Stetson: Holographic Vibration Analysis Study of a 32" Diameter Jet Engine Fan Assembly. Rep. N292720-1, United Aircraft Research Laboratories, Sept. 1974.

Table I. - Chemical Composition of Pertinent Materials

(Percent by weight)

	17-4 PH (AMS 5355)		Stellite 31 (AMS 5382)		IN-100 (AMS 5397)	
	Minimum	Maximum	Minimum	Maximum	Minimum	Maximum
Iron	Balance	Balance	-----	2.0	0	1.0
Cobalt	-----	-----	Balance	Balance	13.0	17.0
Nickel	3.0	5.0	9.5	11.5	Balance	Balance
Chromium	15.50	17.50	24.5	26.5	8.0	11.0
Aluminum	-----	-----	-----	-----	5.0	6.0
Titanium	-----	-----	-----	-----	4.5	5.0
Molybdenum	-----	-----	-----	-----	2.0	4.0
Vanadium	-----	-----	-----	-----	.7	1.2
Boron	-----	-----	-----	-----	01	.02
Carbon	-----	.08	.45	.55	.15	.20
Manganese	-----	1.00	-----	1.00	-----	.10
Sulfur	-----	.04	-----	.04	-----	.015
Silicon	-----	1.00	-----	1.00	-----	.15
Tungsten	-----	-----	7.0	8.0	-----	-----
Phosphorous	-----	.04	-----	.04	-----	-----
Copper	3.00	5.00	-----	-----	-----	-----
Columbium } Tantalum	.15	.45	-----	-----	-----	-----

E-8441

Table II. - Design Dimensions of Various Vane and Blade Airfoils at Hub and Tip Sections

(All dimensions in cm (in.))

Stage	Hub				Tip				Span at midchord	Tip diameter at midchord
	Maximum thickness	Chord length	Leading edge radius	Trailing edge radius	Maximum thickness	Chord length	Leading edge radius	Trailing edge radius		
Compressor rotor										
1	0.267 (0.105)	3.193 (1.257)	0.036 (0.014)	0.048 (0.019)	0.130 (0.051)	3.218 (1.267)	0.018 (0.007)	0.018 (0.007)	4.567 (1.798)	19.76 (7.78)
2	0.330 (0.130)	2.365 (0.931)	0.043 (0.017)	0.066 (0.026)	0.102 (0.040)	2.372 (0.934)	0.018 (0.007)	0.018 (0.007)	3.426 (1.349)	19.96 (7.86)
3	0.183 (0.072)	1.938 (0.763)	0.030 (0.012)	0.041 (0.016)	0.091 (0 036)	1.946 (0.766)	0.018 (0.007)	0.018 (0.007)	2.522 (0.993)	20.34 (8.01)
4	0.163 (0.064)	1.872 (0.737)	0.023 (0.009)	0.025 (0.010)	0.094 (0.037)	1.875 (0.738)	0.018 (0.007)	0.018 (0.007)	1.946 (0.766)	20.65 (8.13)
Compressor stator										
1	0.112 (0.044)	1.989 (0.783)	0.018 (0.007)	0.018 (0.007)	0.224 (0.088)	2.54 (1.000)	0.038 (0.015)	0.028 (0.011)	3.795 (1.494)	19.81 (7.80)
2	0.112 (0.044)	1.781 (0.701)	0.018 (0.007)	0.018 (0.007)	0.185 (0.073)	1.999 (0.787)	0.028 (0.011)	0.023 (0.009)	2.741 (1.079)	20.24 (7.97)
3	0.127 (0.050)	1.654 (0.651)	0.018 (0.007)	0.018 (0.007)	0.178 (0.070)	1.651 (0.650)	0.023 (0.009)	0.023 (0.009)	2.207 (0.869)	20.57 (8.10)
4	0.127 (0.050)	1.676 (0.660)	0.018 (0.007)	0.018 (0.007)	0.180 (0.071)	1.676 (0.660)	0.023 (0.009)	0.023 (0.009)	1.778 (0.700)	20.85 (8.21)
Turbine rotor										
1	0.363 (0.143)	2.121 (0.835)	0 079 (0.031)	0.038 (0.015)	0.160 (0.063)	1.857 (0 731)	0.051 (0.020)	0.038 (0.015)	4.191 (1.65)	24.59 (9.68)
Turbine stator										
1	0.414 (0.163)	2.908 (1.145)	0.094 (0.037)	0.038 (0.015)	3.993 (1.572)	2.192 (0.863)	0.094 (0.037)	0.038 (0 015)	3.962 (1.560)	24.49 (9.64)

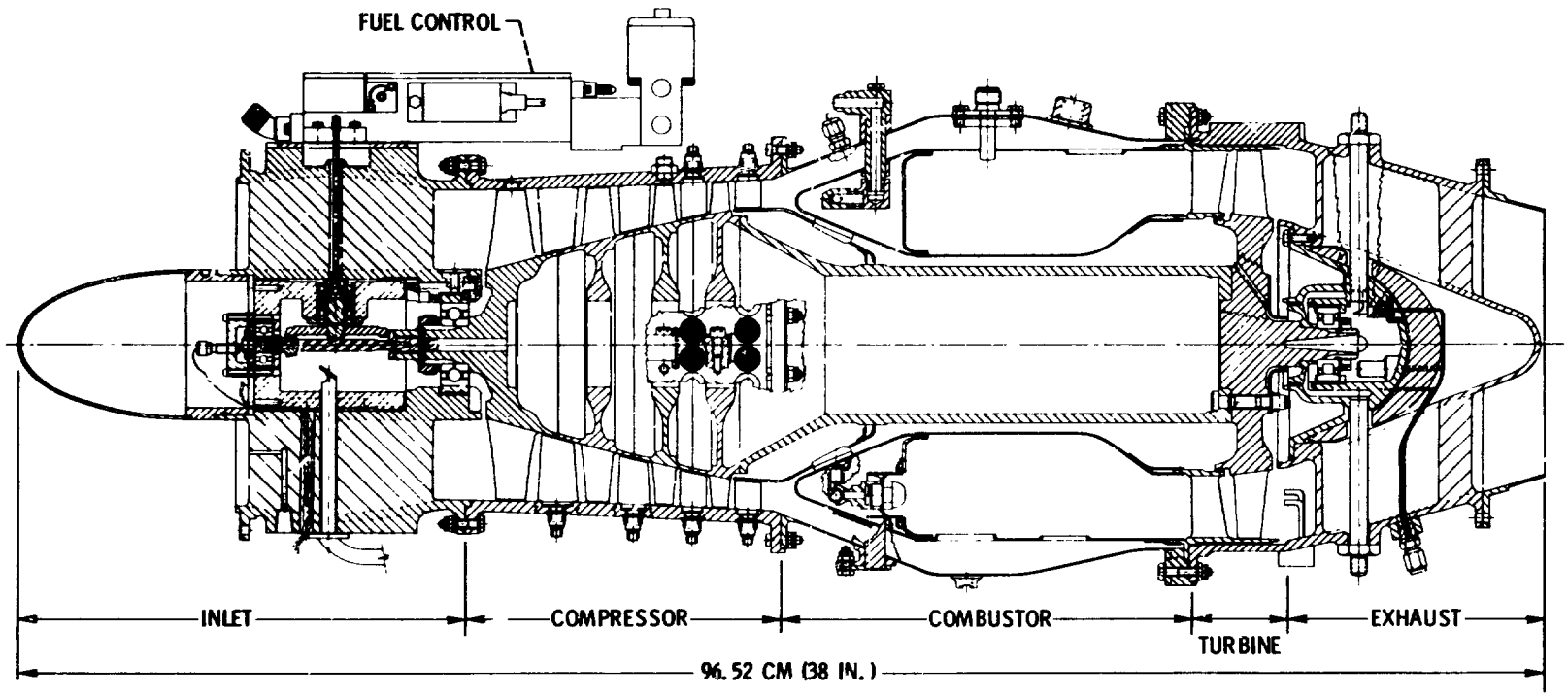

Figure 1. - Cross-sectional view of engine design.

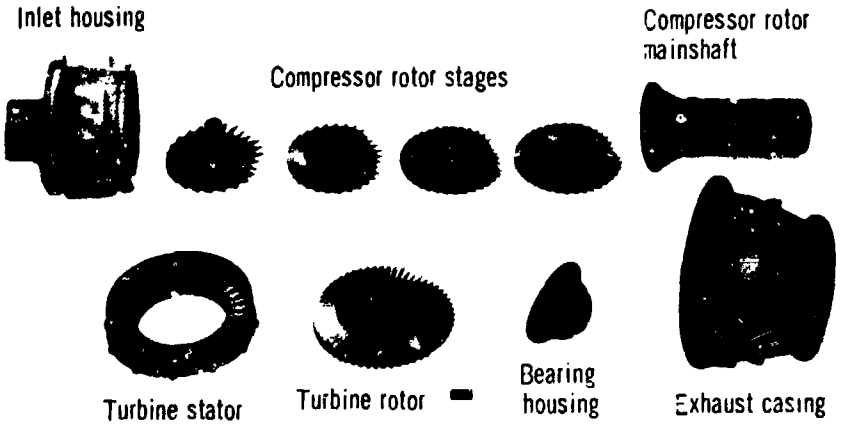

Figure 2. - Castings of major components for small-engine design.

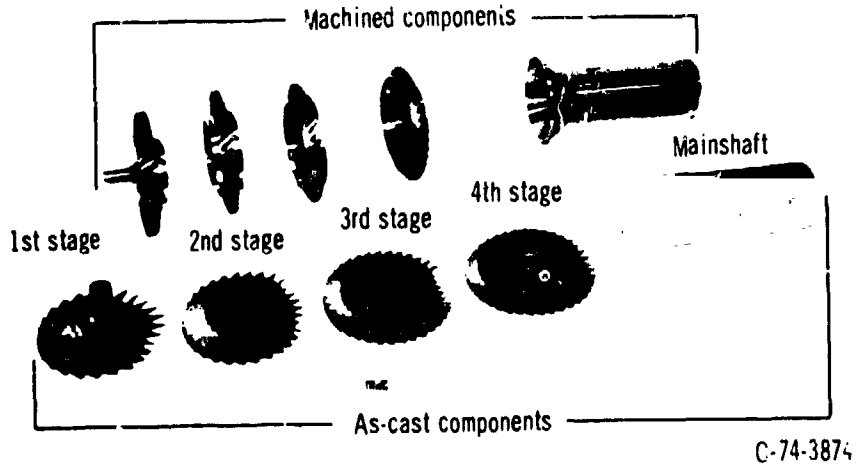

Figure 3. - Comparison of compressor rotor components in "as cast" condition and machined for welding operations.

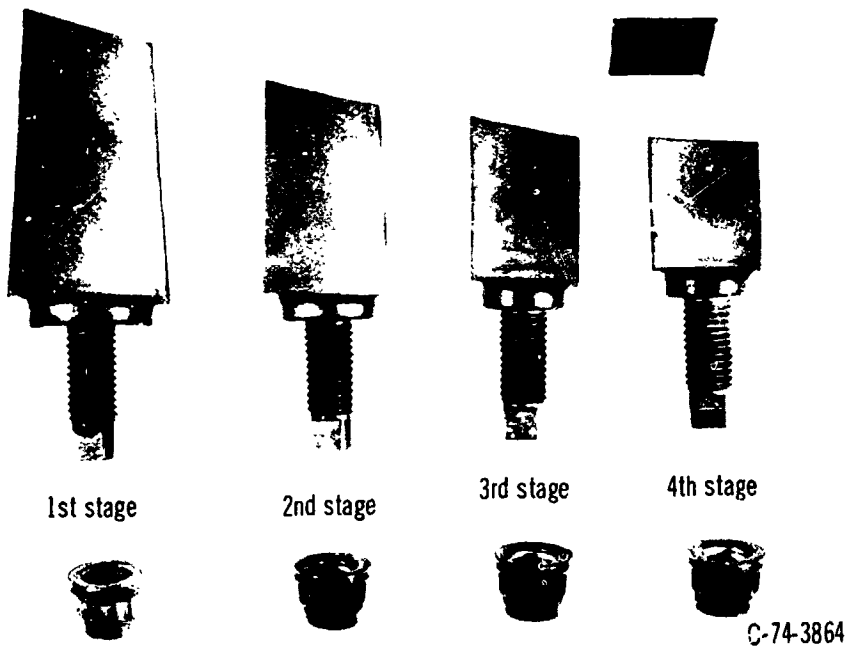

Figure 4. - Individual vanes from each of four compressor stator stages.

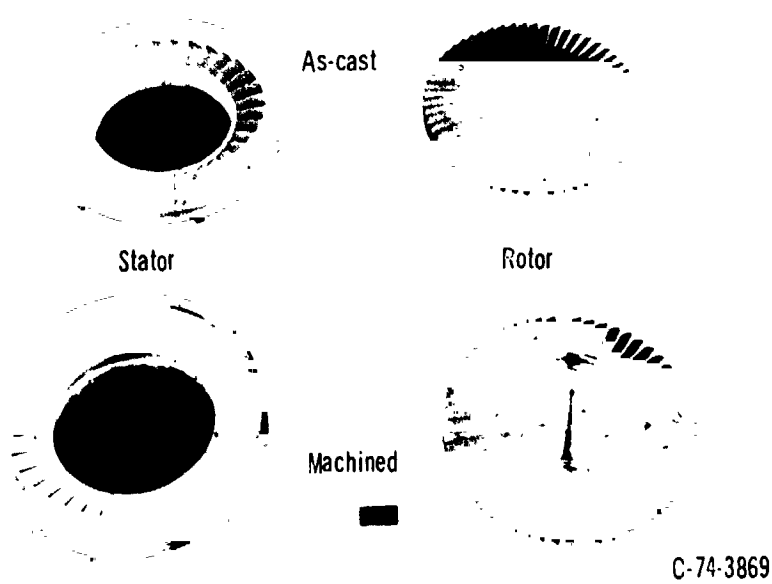

Figure 5. - Comparison of turbine components in the "as cast" condition and the machined version.

Figure 6. - Assembled engine ready for shipment.

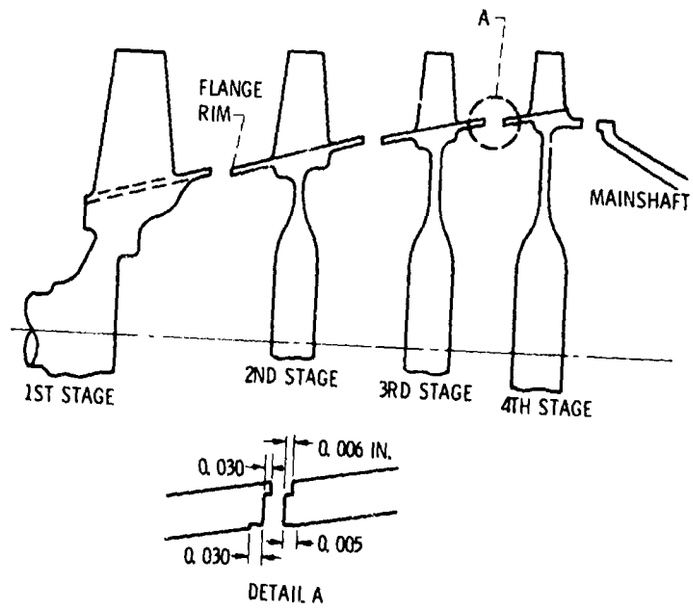

Figure 7. - Cross-sectional view of compressor rotor stages prior to welding.

Figure 8. - View of electron beam weld joining rotor mainshaft to compressor fourth stage rotor

Figure 9 - All-welded compressor rotor assembly

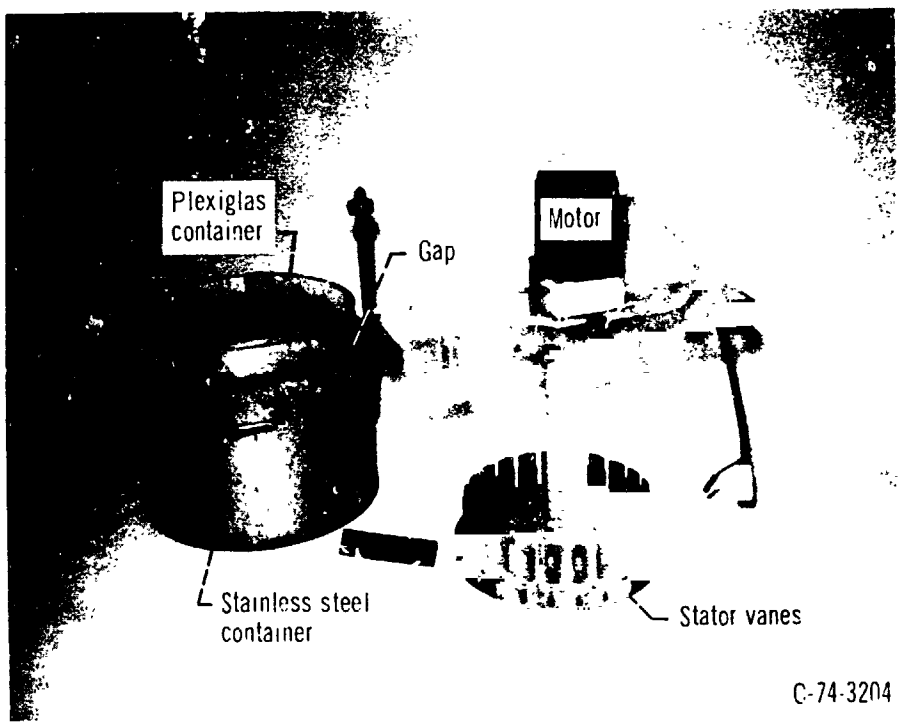

(a) Stator vane milling.

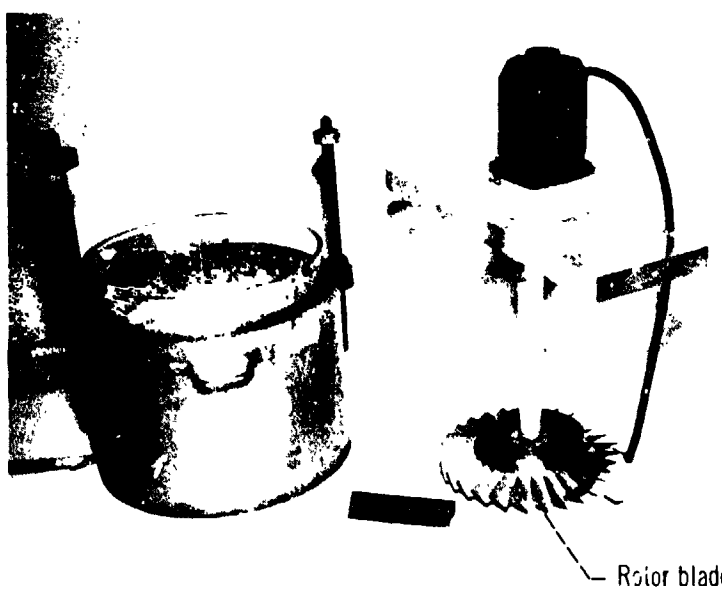

(b) Rotor blade milling.

Figure 10. - Apparatus used for chemical milling compressor airfoils.

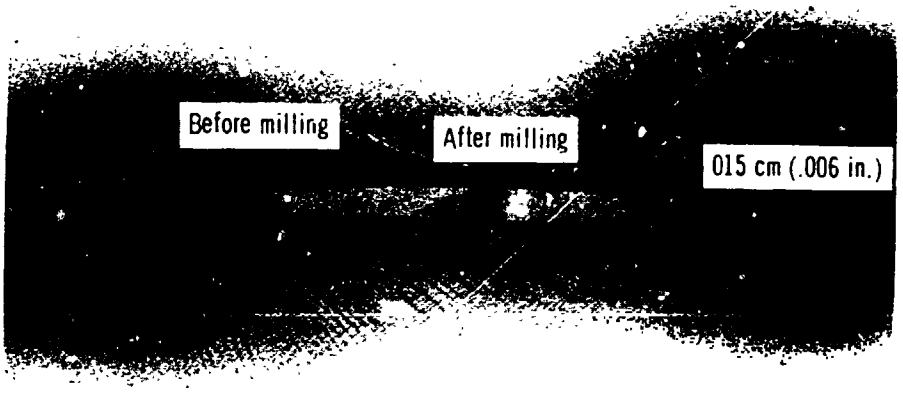

C-75-1968

Figure 11. - Overlay of "eyelash" profiles for tip section of first stage rotor blade before and after chemical milling operation. Section F-F (tip) (9.80 cm radius).

E-8441

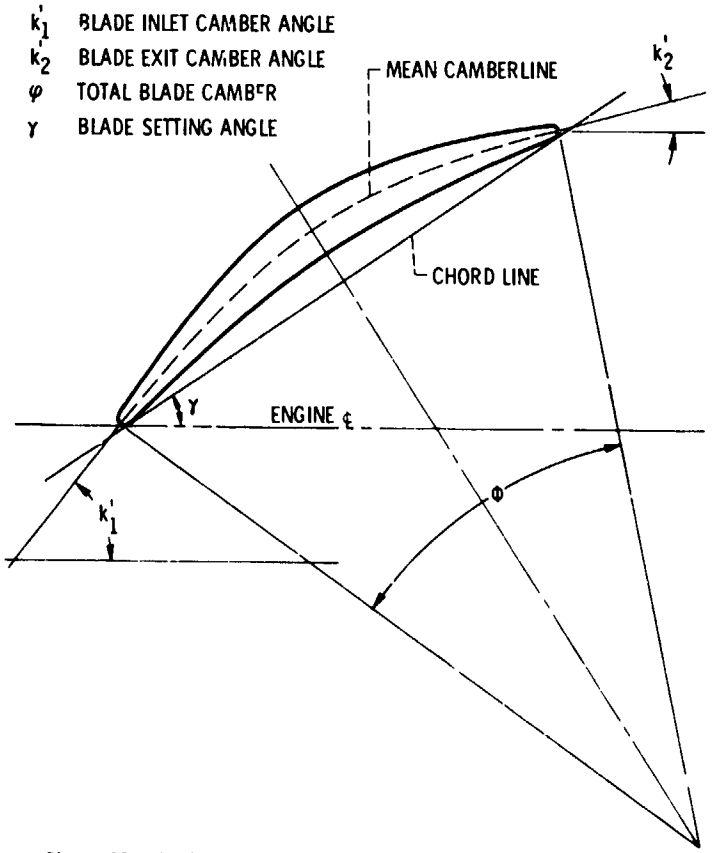

Figure 12. - Typical blade section illustrating blade camber and blade setting angles.

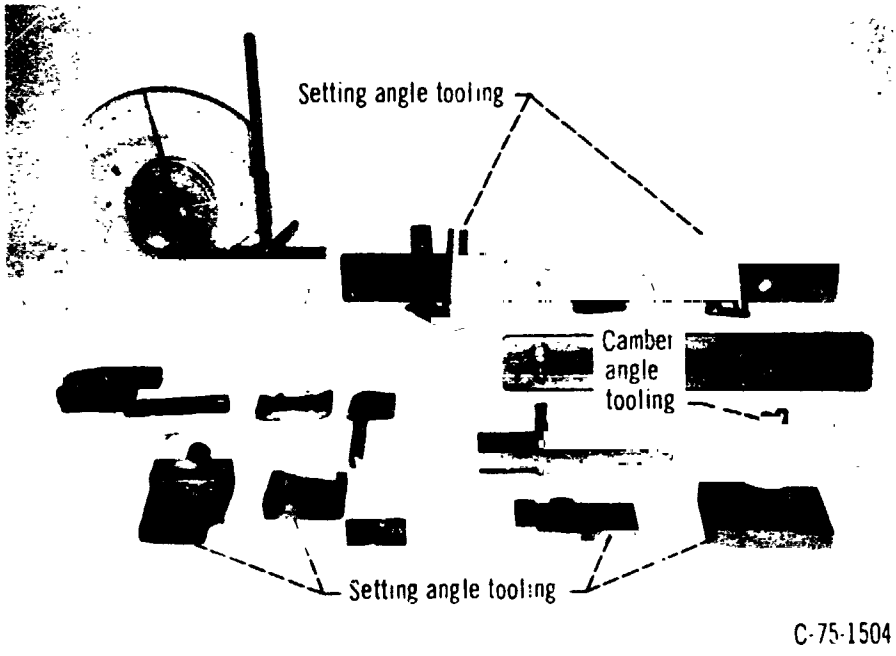

Figure 13. - Tooling developed for affecting compressor rotor blade angle changes.

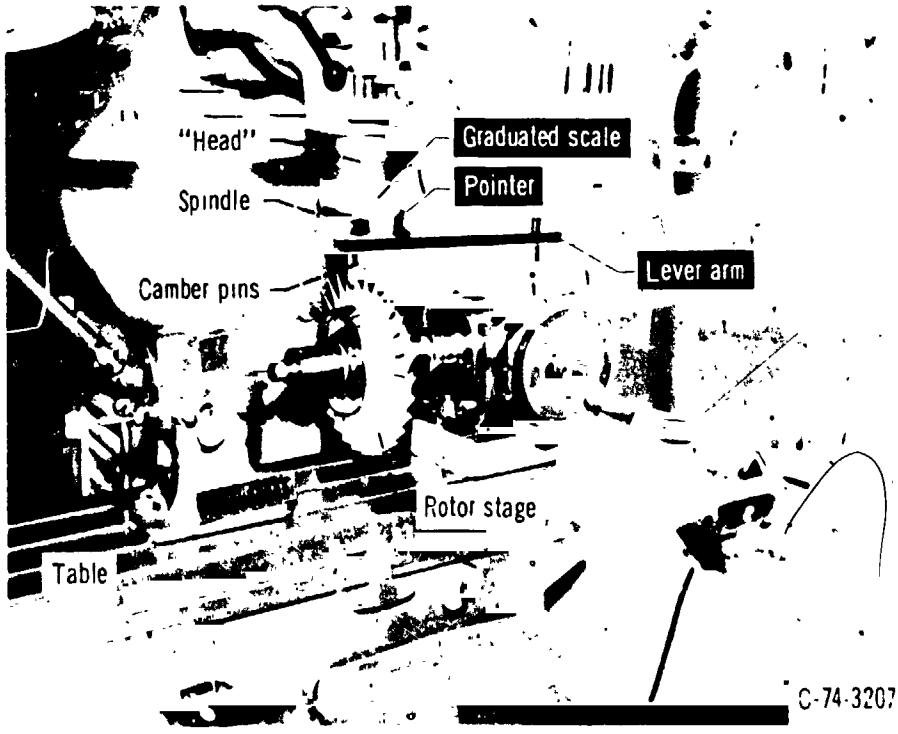

Figure 14. - Typical set-up for affecting angular change in blade camber in compressor rotor stages.

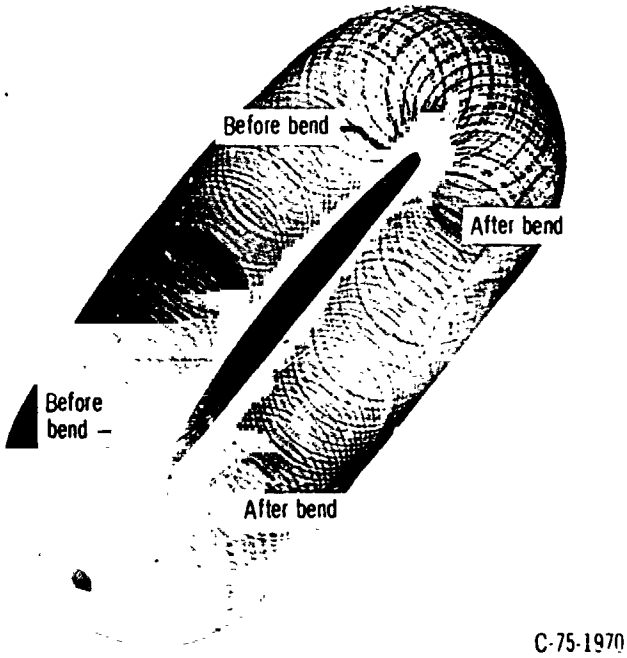

C-75-1970

(a) Section B-B (hub) (8.67 cm radius).

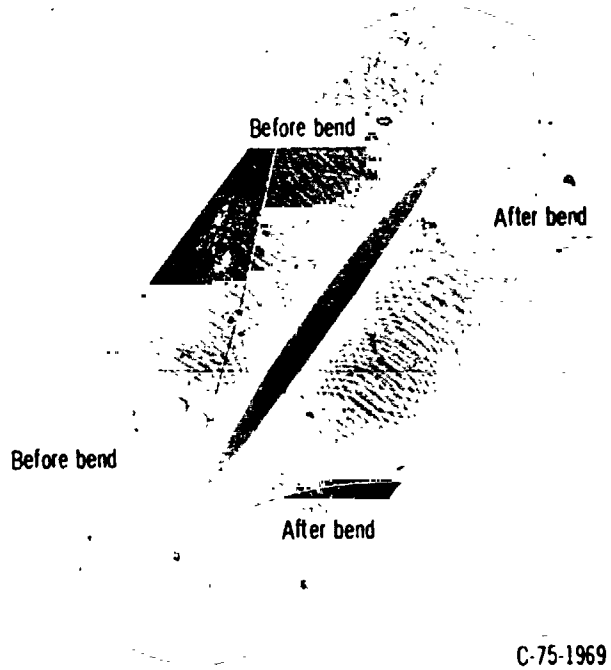

C-75-1969

(b) Section D-D (midspan) (9.51 cm radius).

E-8441

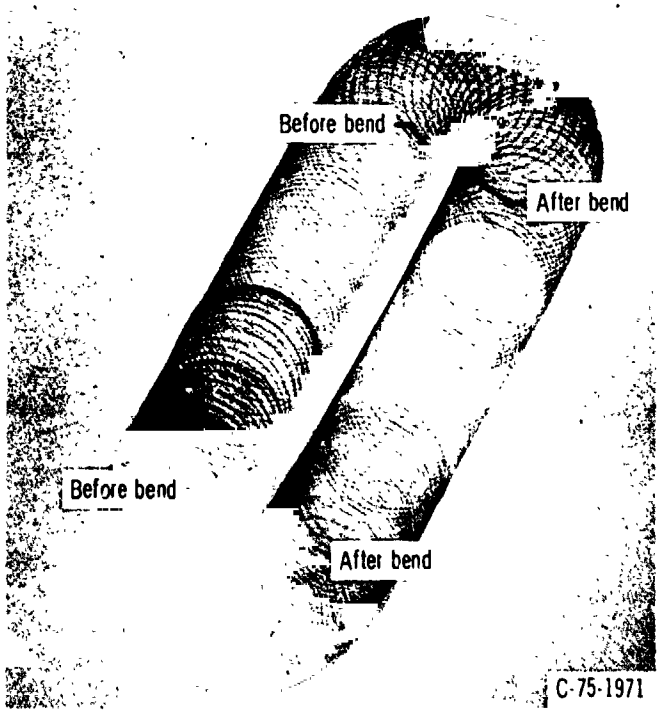

C-75-1971

(c) Section F-F (tip) (10.35 cm radius).

	Exit camber angle, k_2	
Section	Before bend	After bend
B-B	45.0	44.0
D-D	54.1	52.3
F-F	58.5	56.7

	Inlet camber angle, k_1	
Section	Before bend	After bend
B-B	52.1	56.7
D-D	56.7	60.5
F-F	60.6	64.3

Figure 15. - Overlays of "eyelash" profiles at selected sections of a fourth stage rotor blade before and after blade camber angle change.

Section	Setting angle, δ	
	Before bend	After bend
C-C	31.5°	30.9°
F-F	56.3°	51.9°

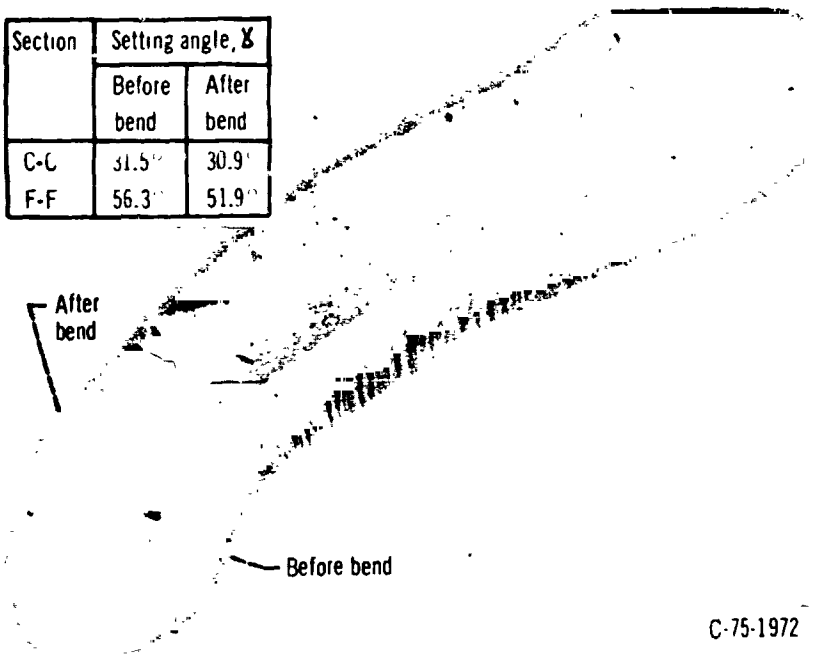

(a) Section C-C (hub) (6.07 cm radius).

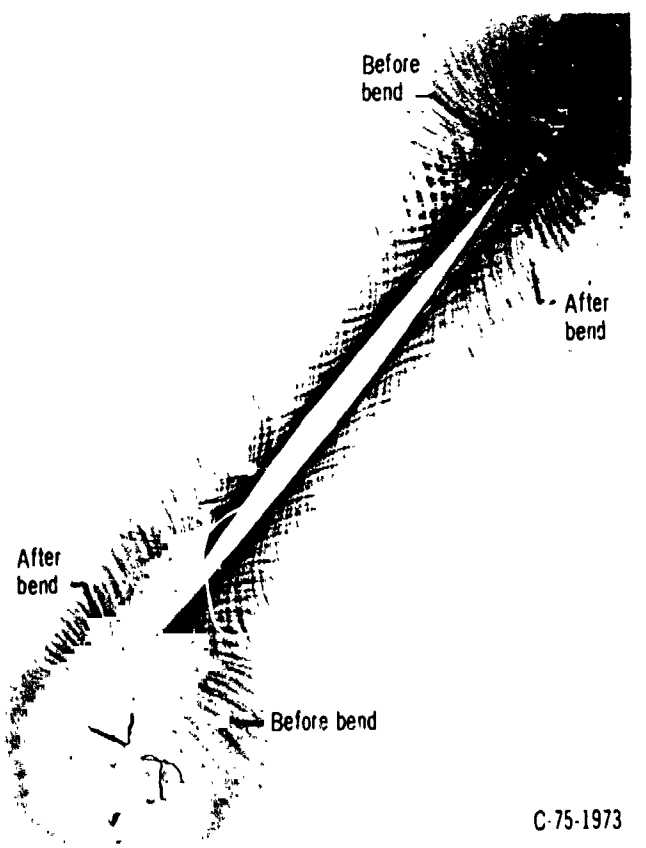

(b) Section F-F (tip) (9.80 cm radius).

Figure 16. - Overlays of "eyelash" profiles at selected sections of a first stage rotor blade before and after blade setting angle change.

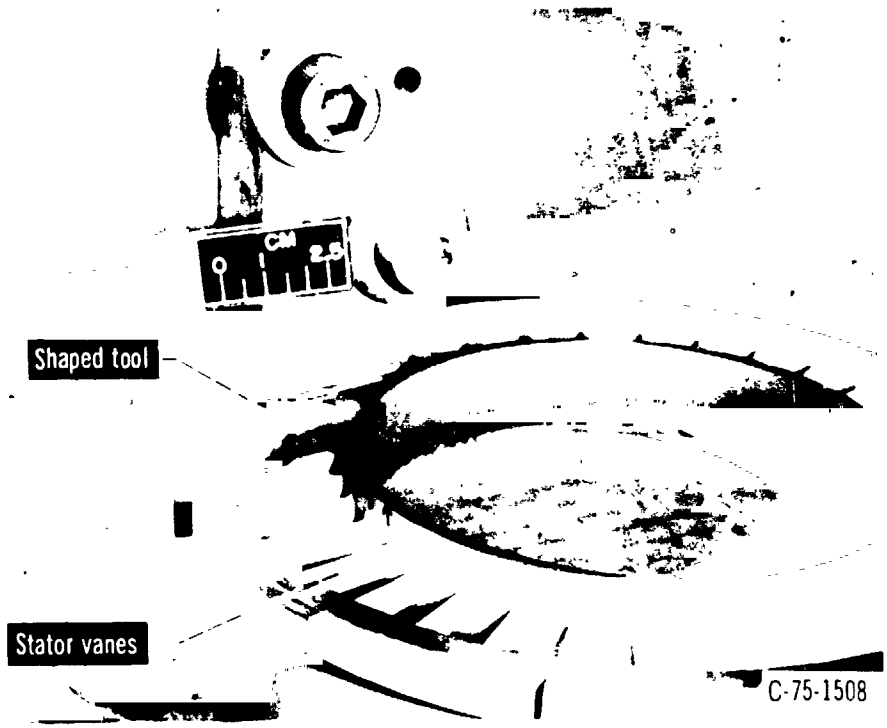

Figure 17. - Apparatus used to perform operation to increase turbine stator throat area.

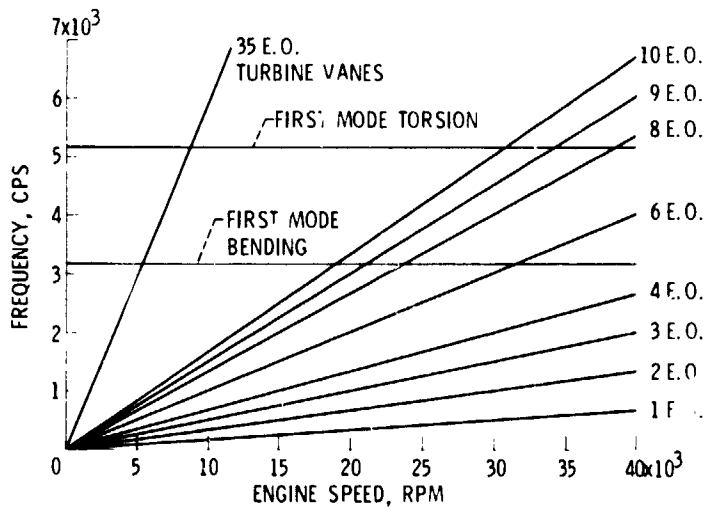

Figure 18. - Turbine rotor blade interference diagram.

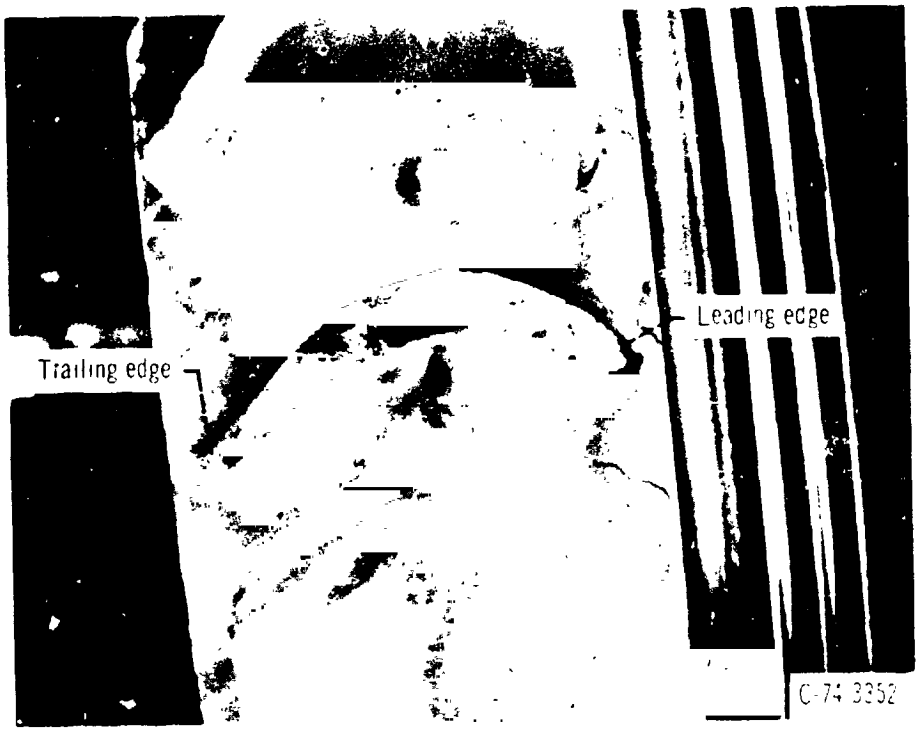

Figure 19 - Fracture-surface of failed turbine blade.

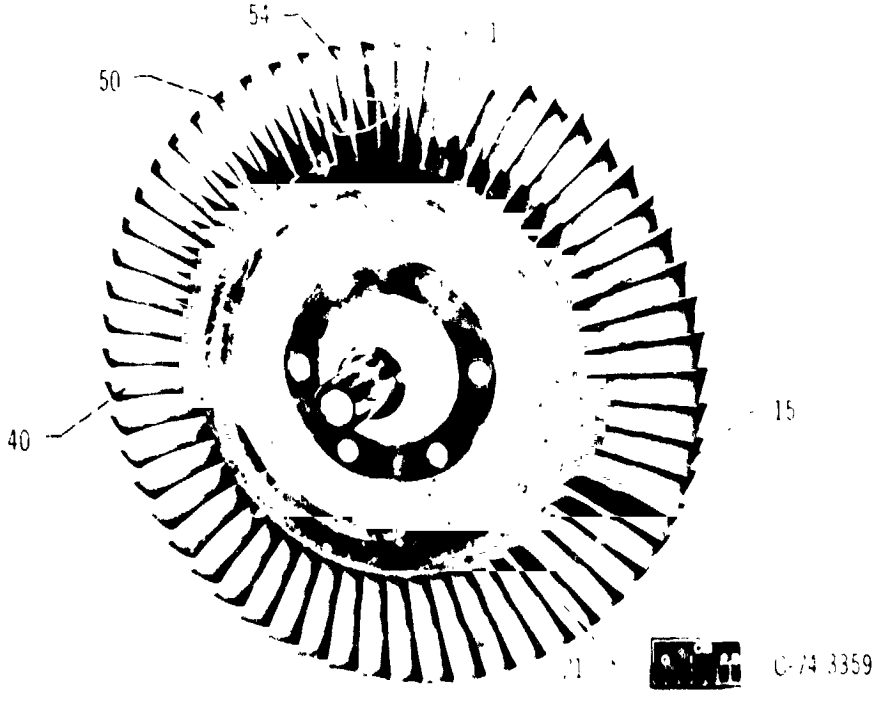

Figure 20. - Turbine rotor showing location of failed blade and those with cracks in the trailing edge

Figure 21 Close up view of crack in trailing edge of Blade No 21

Figure 22 - Apparatus used for [illegible] of turbine blade and turbine rotor

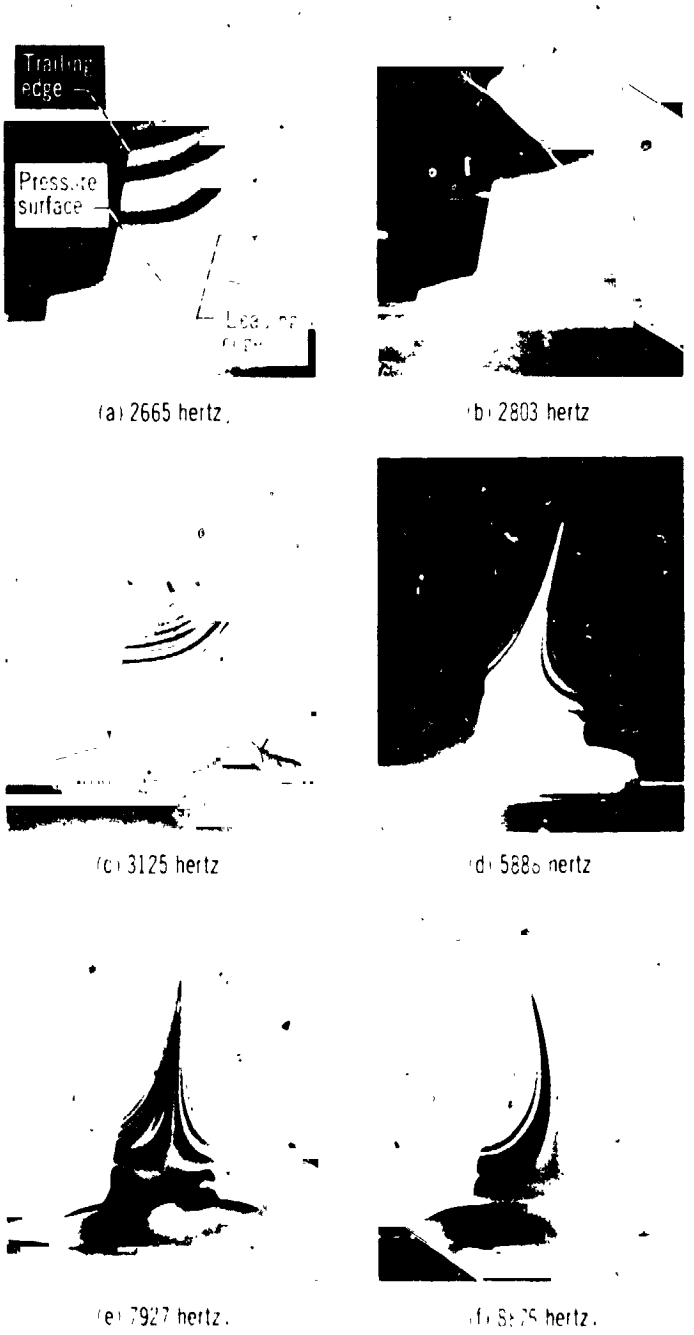

(a) 2665 hertz.

(b) 2803 hertz

(c) 3125 hertz

(d) 5886 hertz

(e) 7927 hertz.

(f) 8275 hertz.

Figure 23 - Turbine blade holograms for various excitation frequencies

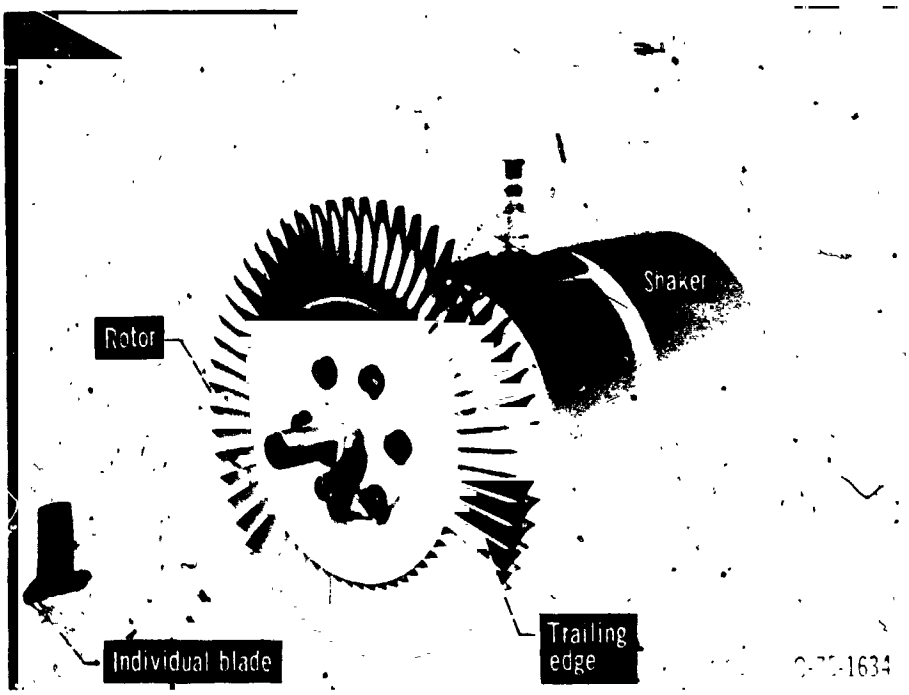

Figure 24. - Turbine wheel mounted on vibration exciter